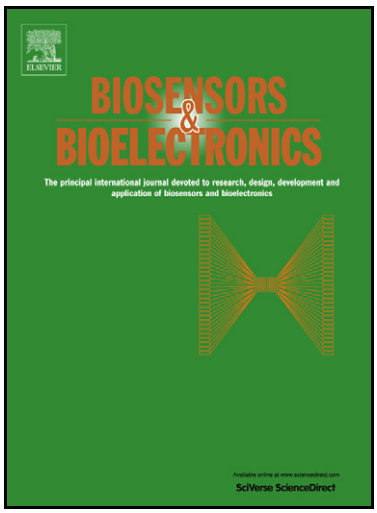

www.elsevier.com/locate/bios

An electrochemical biosensor for ascorbic acid based on carbon-supported PdNi nanoparticles

Xin Zhang, Yang Cao, Sha Yu, Fengchun Yang, Pinxian Xi

PII: S0956-5663(13)00023-7
DOI: http://dx.doi.org/10.1016/j.bios.2013.01.020
Reference: BIOS5687

To appear in: *Biosensors and Bioelectronics*

Received date: 31 October 2012
Revised date: 21 December 2012
Accepted date: 9 January 2013

Cite this article as: Xin Zhang, Yang Cao, Sha Yu, Fengchun Yang and Pinxian Xi, An electrochemical biosensor for ascorbic acid based on carbon-supported PdNi nanoparticles, *Biosensors and Bioelectronics,* http://dx.doi.org/10.1016/j.bios.2013.01.020

An electrochemical biosensor for ascorbic acid based on carbon-supported PdNi nanoparticles

Xin Zhang[b], Yang Cao[a], Sha Yu[a], Fengchun Yang*[a], and Pinxian Xi*[c],

[a] *Key Laboratory of Synthetic and Natural Functional Molecule Chemistry of Ministry of Education, College of Chemistry and Materials Science, Northwest University, Xi'an, Shaanxi, 710069, China*

E-mail: fyang@nwu.edu.cn

Fax: +86 29 88302604; Tel: +86 29 88302604

[b] *Institute of Analytical Science/Shaanxi Provincial Key Laboratory of Electroanalytical Chemistry, Northwest University, Xi'an, Shaanxi, 710069, PR China*

[c] *Key Laboratory of Nonferrous Metal Chemistry and Resources Utilization of Gansu Province, State Key Laboratory of Applied Organic Chemistry and Colleague of Chemistry and Chemical Engineering, Lanzhou University, Lanzhou 730000, P. R. China.*

E-mail: xipx@lzu.edu.cn

Fax: +86 931 8912582; Tel: +86 931 8912589

Abstract

Carbon-supported PdNi nanoparticles (PdNi/C) were synthesized using a novel synthetic route, and characterized by transmission electron microscopy (TEM) and X-ray diffractometer (XRD). The overall metallic content (Pd + Ni) was 10% (w/w) and uniformly distributed in the carbon black (90%) matrix. The electrocatalytic performance of the PdNi/C modified glassy carbon electrode (GCE) was investigated for ascorbic acid (AA) oxidation, and show better catalytic activity than an equal amount of commercially available palladium carbon catalyst. The oxidation potential of AA was negatively shifted to -0.05 V. The biosensor tolerated a wide linear concentration range for AA, from 1.0×10^{-5} M to 1.8×10^{-3} M (R = 0.9973), with a detection limit of 0.5 μM (S/N = 3). Our results demonstrate that The PdNi/C nanomaterials has excellent AA sensing capability, including a fast response time, high reproducibility and stability, with great promise in the quantification of AA in real samples. These qualities make the Pd-based bimetallic catalysts a promising candidate for amperometric sensing.

Keywords:

Pd; Ni; ascorbic acid; electrochemical sensor.

1. Introduction

Ascorbic acid (AA), also known as vitamin C, is commonly used in large scale as an antioxidant in food, animal feed, pharmaceutical formulations, and cosmetic applications [Andre et al., 2010]. Meanwhile, AA plays a key role in many biological processes such as free radical scavenging, cancer prevention and immunity improvement [Kalimuthu and John, 2009]. Especially in central nervous system, AA has important regulative effects on neurotransmitters, enzymes and neuropeptides, and also reflects their level, release and function correspondently. Due to the concentration of AA as mM level in central nervous system and much less in other humoral fluids, the development of a simple and rapid method for the determination of AA with high selectivity and sensitivity is desirable not only for biomedical chemistry and diagnostic, but also for neurochemistry and pathological researches[Ping et al, 2012].

Several methods such as electrophoresis [Wu et al, 2007; Szantai et al, 2004], fluorescence [Wu et al, 2003], chemiluminescence [Anastos et al, 2004; Chen et al, 2010], UV spectroscopy [Fraisse et al., 2002], liquid chromatography [Nováková et al, 2009; Hubbard et al, 2010] and electrochemical methods [Kumar et al, 2008; Ragupathy et al, 2010; Wen et al, 2010; Qiu et al, 2011; Lakshmi et al, 2011] have been reported for the determination of AA. Among them, electrochemical methods are considered to be one of the most potential approaches because of their low cost, high sensitivity and simplicity. However, direct oxidation of AA at bare electrodes is irreversible and the subsequent hydrolysis product, 2, 3-diketogluconic acid [Prieto et al, 1998], is readily adsorbed onto the electrode surface, which results in electrode fouling with high overpotential, poor reproducibility, low selectivity and sensitivity. In addition, some of biological molecules, e.g. dopamine and uric acid, undergo oxidation within same potential window as AA. Therefore, modification of bare electrodes with nanomaterials as the redox active site to make the selective detection of AA accurately and sensitively has been a major goal of much research [Ragupathy et al, 2010; Wen et al, 2010].

Recently, noble metal nanoparticles (such as Au, Ag, Pt, Pd, Ru and their alloys) have emerged as a new class of compounds and received increasing attention [Wu et al, 2012] owing to their unique electrical, magnetic, optical, and catalytic properties. Among them, Pd-based catalysts have become a hot topic of interest because of their more abundance and lower cost in comparison with Pt catalysts [Wen et al, 2010; Zhang et al, 2012]. But many of the pure metals (including palladium) exhibit unsatisfactory sensitivity, poor selectivity and easy poisoning by adsorbed intermediates, which are a critical issue for practical applications [Singh et al, 2010]. The aim of recent work, therefore, is to enhance the sensitivity/selectivity of the sensor by investigating more active and lower cost replacements to pure Pd, hence the interest in bimetallic systems, which bringing interesting physical and chemical properties into effect from the inter-metallic combinations of different metals

[Ferrando et al, 2008; Lim et al, 2009]. The hetero-metallic bond formation with the introduction of a second metal results from the inter-metallic charge transfer or orbital hybridization of the metals. These electronic-structural modifications drastically influence the catalytic performance of the mixed-metal catalyst systems [Stamenkovic et al, 2007; Rodriguez et al, 1992]. In many cases, the hybrid structure alloyed by noble metal and non-noble metals such as iron, cobalt, and nickel not only combines the properties of the individual constituents but also shows an enhancement in specific properties because of the synergistic effects and the rich diversity of the compositions [Bao et al, 2007].

In order to achieve better electrochemical sensor with high sensitivity, selectivity and stability, we have investigated the electrocatalytic activity of PdNi based bimetallic nanomaterials. The choice of the Pd–Ni pair is based on: (i)the information available in literature [Rodriguez et al, 1992; Shen et al, 2010; Liu et al, 2009]; (ii) Ni was found to be a good catalyst [Christoskova et al, 1995], and commonly used as an electrocatalyst for both anodic and cathodic reactions[Fan et al, 1994]; (iii) Ni alloying in the catalyst can improve the hydroxy oxidation by lowering the electronic binding energy[Samant et al, 2005]. (iv) in alkaline media, the presence of Ni oxides provides an oxygen source for oxidation at lower potentials [Zhao et al, 2007], because of the combined effect of the oxygen donation from Ni oxide/hydroxide and the change of electronic structure by electron transfer [Shen et al, 2010], that can greatly enhance the catalytic activity toward oxidation reaction; (v) the inclusion of Ni can provide stability, and minimize the poisoning and cost issues associated with Pd electrodes.

To the best of our knowledge, electrochemical biosensors for AA based on PdNi bimetallic catalysts have not been reported yet. In this paper, PdNi nanoparticles (NPs) are synthesized and dispersed on carbon black to produce PdNi/C, aiming to have a less expensive electrocatalyst for AA. The electrochemical activities of the NPs for AA oxidation are investigated. A comparative study with commercially available palladium carbon (Pd/C) catalysts was also performed using the same conditions for AA electrocatalytic sensing. Results indicate that PdNi/C exhibited a synergistic effect and showed enhanced analytical performance with strong electrocatalytic activity, high sensitivity, stability, and specificity for AA. Its response is rapid with a wide linear range, a low detection limit and good performance in detecting AA content in real commercial sample. These qualities make the PdNi/C electrode a promising candidate for amperometric sensing.

2. Experimental

2.1. Reagents and materials

$PdCl_2$, $Ni(NO_3)_2$, oleylamine (OAm, technical grade, 70%, Aldrich), oleic acid (OA, technical grade, 90%, Aldrich), carbon black (Kejen EC 300J), acetic acid (ACS reagent, g 99.7%, Aldrich). Pd/C (10% Pd loading, $HClO_4$, 70-72%, J. T. Baker) were

purchased and used as received. Nafion (5 wt.%) were purchased from Sigma-Aldrich. AA was from the Chemical Reagent Company of Tianjin (China); 0.1 M KOH and 0.1 M phosphate buffer solution (PBS, pH 7.4) was employed as a supporting electrolyte (50/50, v/v, final pH 11.2). Rod GCEs were from the Chenhua Co. Ltd. (Shanghai, China). All other Chemicals and reagents for electrochemical measurements were of analytical grade and used without further purification. The deionized (DI) water for solution preparation was from a Millipore Autopure system (18.2 MΩ, Millipore Ltd., USA), and all of the solution concentrations have 4 significant digits as standard preparation.

2.2. Preparation of PdNi/C modified GCE

Briefly, PdNi NPs were first prepared by controlled coreduction in oleylamine as a reducing agent and dispersed on carbon black to produce PdNi/C catalysts. Then the PdNi/C as prepared was modified on GCE by general drop-coating method (the detailed preparation process see the Supporting Information).

2.3. Apparatus

All the electrochemical measurements were carried out using a CHI 660D electrochemical workstation (CH Instruments, USA). A conventional three-electrode system, consisting of a modified GCE as the working electrode (working electrode area: 0.071 cm^2), and a saturated Ag/AgCl electrode as a reference electrode, a platinum wire as an auxiliary electrode, was employed. Ag/AgCl and Pt wire were used as the reference electrode and counter electrode, respectively. Electrochemical impedance spectroscopy (EIS) was performed with the same three-electrode configuration in an electrolyte solution of 0.1 M KCl containing 0.01 M $[Fe(CN)_6]^{4-/3-}$, in a frequency range from 1 Hz to 1000 kHz with an AC probe amplitude of 50 mV.

XRD profiles obtained (XRD-6000, Shimadzu) with high-intensity Cu Kα radiation (λ = 1.5406 Å). Morphologies of PdNi NPs were determined using scanning electron microscopy (SEM) (JEOL JEM-2100).

3. Results and discussion

3.1. Characterization of PdNi/C

3.1.1. Structural characterization

The TEM and HRTEM images depicted in Fig. 1 show the direct morphological observations of the as-prepared PdNi NPs. In Fig. 1A, it can be seen that the PdNi NPs are well distributed, with their diameter measured to be 3.6±0.4 nm (Figure 1A). The HRTEM image (Fig. 1B) of the PdNi NPs shows that the interplanar spacing of the particle lattice was 0.229 nm, which agreed with the (1 1 1) lattice spacing of facecentered cubic Pd (0.224 nm). The Selected area electron diffraction (SAED) pattern of a group of a representative single NP indicates that the NPs are highly crystallized. Figure 1D is the HAADF-STEM iamge of PdNi nanocrystals.

To obtain the further crystallographic information of the prepared NPs, an XRD measurement was conducted. The XRD patterns for Pd/C and PdNi/C (Fig. 1E) catalysts both show two diffraction peaks that are indexed to the (1 1 1) and (2 0 0) planes of Pd face-centered cubic (fcc) crystal structure, respectively. Besides that, the diffraction peaks at 21.37° and 23.21° in the PdNi/C catalyst (b) are ascribed to the (1 1 1) and (2 0 0) plane of cubic Ni system. These results reveal the presence of Ni, and the same planes of Ni as Pd indicating that alloying Pd with Ni results in a crystal lattice expansion in PdNi NPs.

3.1.2. Electrochemical characterization

EIS is widely used to study features of electrodes to obtain information on electron transfers between the electrolyte and the electrode surface. The semicircular part at higher frequencies corresponds to the electron transfer limited process, and a linear portion at low frequencies resulting from diffusion limited process. The semicircle diameter equals the electron transfer resistance, R_{ct}. This resistance reveals the electron transfer resistance of the modified layer [Wang et al, 2010]. As shown in Fig. 1F, the Nyquist plot of PdNi/C modified GC, Pd/C modified GC and bare GC electrodes in the frequency range of 1 Hz to 1000 kHz, show a straight line in the low frequency domain and a semicircle in the high frequency domain, wherein, only a part of the semicircles can be seen at high frequency due to the limitation of the electrochemical analyzer used here. These illustrate that both diffusion-limiting and electron-transfer-limiting steps exist for the three electrodes. In the high frequency region, it can be clearly inferred that the sequence of R_{ct} for the three electrodes is PdNi/C < Pd/C < GC electrodes. This demonstrates that the PdNi/C modified GCE has higher electrochemical activity than Pd/C and GCE, indicating that the PdNi/C nanocomposite develops a synergistic effect of Pd and Ni. In other words, the heterogeneous electron transfer capability of Pd NPs has been greatly enhanced by incorporating Ni NPs.

3.2. AA sensing using cyclic voltammetry

3.2.1. Electrocatalytic oxidation of AA

The oxidation of AA at PdNi/C modified GCE were first studied by cyclic voltammetry (CV) in 50 mM KOH+ 50 mM PBS solution containing 10 mM AA. For comparison, the voltammogram of a Pd/C modified GC and bare GC electrodes have also been included in Fig. 2. As it is seen, all of the electrodes exhibited an electrocatalytical oxidation response towards AA, but the anodic peak current at the PdNi/C modified GCE is significantly larger than that at the Pd/C and bare GCE, due to the high electrocatalytic activity of the PdNi/C. Furthermore, the onset of AA oxidation peak of PdNi/C is about -0.41 V, which shows a negative shift compared to that of Pd/C (-0.36 V) and bare GCE (-0.32 V) catalysts. This indicates that the PdNi/C catalyst is able to reduce the overpotential in AA oxidation. A notable difference between the three electrodes was that PdNi/C modified GCE shows another small but sharp peak, which has almost equal potential with voltammogram b. That

may exactly demonstrate the synergistic effect of Ni with Pd. In other word, the first anodic peak of Fig. 2c, corresponds to catalytic activity of Ni hydroxides for AA oxidation as well as the second peak corresponds to Pd oxide NPs.

The probable AA oxidation process on the surface of the PdNi/C modified GCE is as follows:

$$Pd + 2OH^- \longrightarrow Pd\text{-}O + H_2O + 2e^- \quad (1)$$

$$Ni + 2OH^- \longrightarrow Ni(OH)_2 + 2e^- \quad (2)$$

$$Ni(OH)_2 + Pd\text{-}O \longrightarrow NiOOH + Pd \quad (3)$$

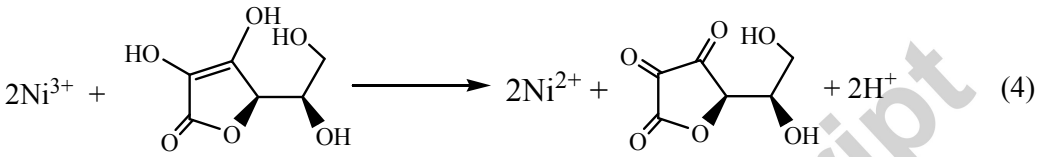

(4)

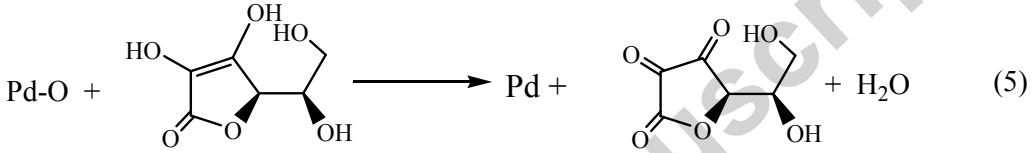

(5)

It is known that AA oxidation is an inner-sphere reaction and the electron transfer kinetics is sensitive to the electrode's surface properties [Wu et al, 2012; Maleki et al, 2006]. Thus, such an enhanced electrocatalytic activity of the PdNi/C catalyst may result from the change in the electron transfer kinetics of Pd, caused by the introduction of Ni. Previous studies [Shen et al, 2010; Wang et al,2008] have revealed that the nickel hydroxides ($Ni(OH)_2$ and NiOOH) have a high electron and proton conductivity, and exhibit a high catalytic activity as heterogeneous catalysts, that has a beneficial effect on hydroxyls oxidation in alkaline media. Here, the nickel hydroxides, the main component of the Ni species, may chiefly account for the great promotion of AA oxidation on Pd in alkaline media through the reversible redox, according to Eqs. (1) to (5). Pd usually formed inactive oxide Pd-O after adsorption and catalytic reaction of -OH. The Ni $(OH)_2$ transfer the oxygen from Pd–O by the electrochemical oxidation of Ni^{2+} to Ni^{3+} (Eqs. (3)), so, the "clean" Pd surface can react with the -OH afresh, which can greatly facilitate the adsorption process of –OH on Pd surface. Then an electrocatalytic process initiated (Eqs. (4)) by the oxidation of AA adsorbed on the Ni^{3+} surface and the regeneration of Ni^{2+}, which can be used to "clean" the Pd–O surface again (Eqs. (3)).

In addition, the smaller particles size and high electrochemically active surface area of the bimetallic systems are also need to be considered for the higher electrocatalytic activity of PdNi/C than Pd/C, which will be discussed in section 3.3.2 later. All the above analysis results confirmed that Pd have a larger utilization in synergistic effect with Ni.

3.2.2. Effect of scan rate of AA

Fig. 3A shows the cyclic voltammograms of the PdNi/C modified GCE in the presence of 2.0 mM AA at various scan rates. As is obvious, both the oxidation peak current and oxidation peak potential were observed to increase with increasing scan rate from 20 to 100 mV/s. This result suggests a kinetic limitation in the reaction between redox sites of the PdNi/C modified GCE and AA. Meanwhile, the anodic peak current is proportional to the square root of the scan rate (Fig. 3B), indicating a typical behavior for a mass transfer controlled reaction.

In order to get information on the rate-determining step, a plot of E_p vs. log ν (Fig. 3C) revealed a linear behavior with a slope 62.0 mV, obeying the following equation, which is valid for a totally irreversible diffusion controlled process [Shamsipur et al, 2010]:

$$E_p = b/2 \log \nu + \text{constant} \quad (6)$$

where E_p and b indicate the oxidation peak potential and the Tafel slope, respectively. Thus, based on this equation and a slope of 62.0, the Tafel slope b was calculated as 124.0 mV. This slope indicates the fact that a one-electron transfer process should be rate-limiting step, assuming a transfer coefficient of α=0.47, instead of two-electron and one-proton process suggested by other literature. However, this is very consistent with our expected mechanism from Eqs. (1) to (5), and demonstrate the small sharp peak was not second-electron transfer process of AA, but that the synergistic effect of Ni with Pd (Eqs. (4)).

3.2.3. Influence of AA concentration

Effect of AA concentration on the anodic peak current for its electrocatalytic oxidation at the modified electrodes was also investigated by cyclic voltammetry. Fig. S1 illustrates a series of cyclic voltammograms of PdNi/C modified GCE in the presence of different concentrations of AA ranging from 0 to 10 mM in 50 mM KOH+ 50 mM PBS solution, and the correlation between the oxidation peak intensity and AA concentration is shown in inset of Fig. S1. As is obvious, the anodic peak current increased constantly with increasing AA concentration, and the plot is linear up to a concentration of 10 mM. The linear regression equation was expressed as:

$$I\ (\text{mA}) = 0.0217 + 0.03803 C_{AA}\ (\text{mM})\ (R^2 = 0.9881),$$

The current deviates from linearity at higher AA concentrations, most possibly due to the saturation of active sites at the surface of electrode and the passivation of the electrode and/or the formation of 2,3-diketogluconic acid, as this is known to occur in alkaline media [Prieto et al, 1998].

3.3. Amperometric response of AA

3.3.1. Sensor optimization and calibration

Fig. 4A shows the amperometric responses measured to investigate the electroactivity of PdNi/C modified GCE towards dropwise addition of 0.2 mM AA under different detecting potentials from -0.40 to 0.00 V in 50 mM KOH+ 50 mM PBS. In general, the current response increased with the applied potential. The current

response reached the maximal value at -0.05 V, which even exceeded the current response at 0.00 V. We thought it may be attributed to the faster rate and stronger driving force promoted by the little overpotential. Therefore, -0.05 V was selected as the optimal constant detecting potential, not only because it generated a high enough signal but also because it was relatively lower. High potentials might oxidize some interfering species that are not reactive under low potentials.

Fig. 4B shows the amperometric response of PdNi/C modified GCE with successive additions of AA at -0.05 V. As AA was added to the stirring solution, PdNi/C modified GCE responded rapidly to the substrate and achieved steady-state current within 2 s. The calibration curve for the PdNi/C modified GCE is shown in the inset of Fig. 4B. A good linear relationship ($i(mA) = 0.054C_{AA} - 0.0031$, $R^2 = 0.9973$) was exhibited and its concentration in the range of 10 μM to 1.81 mM, with a detection limit of 0.5 μM based on S/N = 3. The sensitivity was calculated to be 760.6 μA mM cm^{-2}. The performance of our PdNi/C modified GCE sensor is compared with those of other published AA sensors based on applied potential, linear range, detection limit, and sensitivity, which are listed in Table S1. It can be observed that our sensor exhibits a very high sensitivity, low operational potential, excellent detection limit and wide linear range. These are absolutely owing to the synergistic effects of Pd and Ni, which facilitates high catalytic activity towards AA and large active surface area.

3.3.2. Chronoamperometric studies

Chronoamperometry was employed for the investigation of real surface area of the modified electrodes. The real surface of electrode is an effective parameter in determining the peak currents in catalytic redox reactions. Fig. S2 shows the chronoamperometric measurements of AA at the Pd/C and PdNi/C modified GC electrodes in solutions containing 0.01 M AA and 50 mM KOH+ 50 mM PBS, at a fixed potential of -0.05 V. Under the diffusion controlled conditioned and according to the Cottrell equation the current intensity is given by [Bard et al, 2001]:

$$I = nFAD^{1/2}C^{*}/\pi^{1/2}t^{1/2} \qquad (7)$$

where A is real surface area, D is diffusion coefficient and C^{*} is the bulk concentration of AA. According to Cottrell equation, the slope of a linear plot of I vs. $t^{-1/2}$ can be used for the estimation of the real surface area of the electrodes, A. The slopes of these plots, shown in the insets of Fig. S2 for the Pd/C and PdNi/C modified GC electrodes, respectively, revealed that the surface area of PdNi/C modified GCE is 3.4 times larger than that of the Pd/C. That may be due to the phenomenon bimetallic NPs were significantly smaller than monometallic NPs, which relate to the competitive nucleation process of the particles [Ren et al, 2007] and exist higher specific surface area for catalysis. This can explain clearly the synergistic effect of Pd and Ni on the enhancement of electrocatalytic currents in another aspect.

3.4. Sensor stability and specificity

The stability of the sensor was investigated by measuring its sensitivity (S) over three weeks under ambient conditions during which the sensor retained 85.6% of its

original sensitivity (S_o) (Fig. S3A). The PdNi/C modified GCE response was stable over a long operational period of 50 min for 0.2 mM AA in 50 mM KOH+ 50 mM PBS with a loss of 49.5% in the current signal (Fig. S3B). The current responses for real AA sample of vitamin C tablets were measured 3 times using the same electrode with only a relative standard deviation (RSD) of 1.8 % (Fig. S3C). These results confirm that the PdNi/C modified GCE has a high stability as well as good reproducibility those make it applicable for practical use.

The specificity of the sensor was investigated using different interferents that normally co-exist with AA in human blood serum and other samples. In the present work, the interference experiments were carried out by successive addition of 0.2 mM AA and 0.20 mM interfering species (Glucose, Fructose, Lactose, Sucrose, UA, DA Glycine, Tryptophan, $NaNO_2$) in 50 mM KOH+ 50 mM PBS. The measured effects of different interferents along with AA at -0.05 V are shown in Fig. 5. For all the interfering species, PdNi/C modified GCE did not show any significant fluctuation in the sensor response, and the current responses were neglected compared to AA. These results indicate that PdNi/C modified GCE is highly specific to AA in the presence of various organic and inorganic interfering species normally found in food and biological samples at -0.05 V. Furthermore, the current response becomes stable in less than 2 s, which indicates a significantly rapid response of PdNi/C towards AA.

3.5. AA Sample analysis

To verify the practicality of the modified electrode, the PdNi/C modified GCE has been applied to the direct detection of AA in vitamin C tablets. Vitamin C tablets were firstly dissolved in PBS (pH 7.4), and then diluted by KOH. The AA content of the tablet was determined to 0.21 mM using the present electrochemical method (see Fig. S3C), which is in accordance with the result obtained from HPLC (0.20 mM). Known amount of standard AA was added into the diluted (10 times) real sample and recoveries were provided (Table 1). The recoveries are between 95.1% and 98.8% with a relative standard deviation (RSD) less than 2.0%.

The present PdNi/C-based electrochemical sensor can also be applied to detect AA in rabbit and goat serum. The same procedure was carried out as Vitamin C tablets. The AA content was determined to be 0.008 mM for rabbit and 0.004 mM for goat serum, which is also in accordance with the result obtained from HPLC (0.006 and 0.005 mM). The recoveries were 98.5–106.3% for rabbit and 96.9–102.3% for goat serum, with a RSD lower than 1.5–2.0%, showing that PdNi/C modified GCE is reliable for AA analysis in food safety and biological analytical platform. All of these results indicate the present PdNi/C-based electrochemical sensor can be used for the direct detection of AA in practical samples.

4. Conclusions

Carbon-supported PdNi nanoparticles have been prepared by a novel synthetic

route, and have excellent synergistic effects. The PdNi/C modified GCE displayed substantially higher electrocatalytic activity to AA oxidation with a higher current response and lower oxidation potential than commercial Pd/C catalyst with equal metal content. This PdNi/C modified GCE electrochemical sensor has a low detection limit of 0.5 μM and a very high sensitivity of 760.6 μA mM^{-1} cm^{-2}, and its response is linear for up to 10 mM AA concentration. When these superior performance characteristics are combined with ease of fabrication, long-term stability, good reproducibility, rapid response, and excellent specificity to AA in the presence of common interferents, the PdNi/C modified GCE is a potential candidate for routine AA analysis.

Acknowledgements

We gratefully acknowledge support from the Research Fund for the Doctoral Program of China (20126101120012), the Research Plan Projects of Shaanxi Education Department (12JK0578 and 12JK0617), the Research Grant of Northwest University (NF10005) and Open Foundation of Key Laboratory of Synthetic and Natural Functional Molecular Chemistry (Ministry of Education, ZS11034). This work was also supported by the National Natural Scientific Foundation of China (No. 21201092), the Research Funds for the Central Universities (Lzujbky-2012-65) and (Lzujbky-2012-203).

References

Anastos, N., Barnett, N.W., Hindson, B.J., Lenehan, C.E., Lewis, S.W., 2004, Talanta 64, 130.

Andre, C., Castanheira, I., Cruz, J.M., Paseiro, P., Sanches-Silva, A., 2010, Trends Food Sci. Technol. 21, 229.

Bao, J., Chen, W., Liu, T.T., Zhu, Y.L., Jin, P.Y., Wang, L.Y., Liu, J.F., Wei, Y.G., Li, Y.D., 2007, ACS Nano. 1, 293.

Bard, A.J., Faulkner, L.R., Electrochemical Methods, Fundamentals and Applications, Wiley, 2001, New York, 161.

Chauhan, N., Narang, J., Rawal, R., Pundir, C.S., 2011, Synthetic Met. 161, 2427.

Chen, H., Li, R.B., Lin, L., Guo, G.S., Lin, J.M., 2010, Talanta 81, 1688.

Christoskova, St.G., Danova, N., Georgieva, M., Argirv, O.K., Mehandzhiev, D., 1995, Appl. Catal. A 128, 219.

Cui, R.j., Wang, X.Y., Zhang, G.H., Wang, C., 2012, Sens. Actuators B 161, 1139.

Dalmasso, P.R., Pedano, M.L., Rivas, G.A., 2012, Sens. Actuators B 173, 732.

Fan, C., Piron, D.L., Sleb, A., Paradis, P., 1994, J. Electrochem. Soc. 141, 382.

Ferrando, R., Jellinek, J., Johnston, R.L., 2008, Chem. Rev. 108, 845.

Fraisse, L., Bonnet, M.C., de Farcy, J.P., Agut, C., Dersigny, D., Bayol, A., 2002, Anal. Biochem 309, 173.

Hubbard, K.E., Wells, A., Owens, T.S., Tagen, M., Fraga, C.H., Stewart, C.F., 2010, Biomed. Chromatogr, 24, 626.

Kalimuthu, P., John, S.A., 2009, Bioelectrochemistry 77, 13.

Kumar, S.A., Lo, P.H., Chen, S.M., 2008, Biosens. Bioelectron. 24, 518.

Lakshmi, D., Whitcombe, M.J., Davis, F., Sharma, P.S., Prasad, B.B., 2011, Electroanal. 23, 305.

Li, F., Tang, C., Liu, S.F., Ma, G.R., 2010, Electrochim. Acta 55, 838.

Lim, B., Jiang, M.J., Camargo, P.H.C., Cho, E.C., Tao, J., Lu, X.M., Zhu, Y.M., Xia, Y.N., 2009, Sci. 324, 1302.

Liu, Z., Zhang, X.H., Hong, L., 2009, Electrochem. Commun. 11, 925.

Maleki, N., Safavi, A., Tajabadi, F., 2006, Anal. Chem. 78, 3820.

Nováková, L., Solichová, D., Solich, P., 2009, J. Chromatogr. A 1216, 4574.

Ping, J., Wu, J., Wang, Y.X., Ying ,Y.B., 2012, Biosens, Bioelectron. 34, 70.

Prieto, F., Coles, B.A., Compton, R.G., 1998, J. Phys. Chem. B 102, 7442.

Qiu, S., Gao, S., Liu, Q., Lin, Z., Qiu, B., Chen, G., Biosens. 2011, Bioelectron. 26, 4326.

Ragupathy, D., Gopalan, A.I., Lee, K.P., 2010, Sens. Actuators B 143, 696.

Ren, G.Q., Shi, H.L., Xing, Y.C., 2007, Nanotechnology 18, 385604.

Rodriguez, J.A., Goodman, D.W., 1992, Sci.257, 897.

Samant, P.V., Fernandes, J.B., Rangel, C.M., Figueiredo, J.L., 2005, Catal. Today 173, 102.

Shamsipur, M., Najafi, M., Hosseini, M.R.M., 2010, Bioelectrochemistry 77, 120.

Shen, S.Y., Zhao, T.S., Xu, J.B., Li, Y.S., 2010, J. Power Sources 195, 1001.

Shi, W.T., Liu, C.X., Song, Y.L., Lin, N.S., Zhou, S., Cai, X.X., Biosens. Bioelectron. 2012, 38, 100.

Singh, B., Laffir, F.,. McCormac, T, Dempsey, E., 2010, Sens. Actuators B 150, 80.

Stamenkovic, V.R., Mun, B.S., Arenz, M., Mayrhofer, K.J.J., Lucas, C.A., Wang, G.F., Ross, P.

N., Markovic, N. M., 2007, Nat. Mater. 6,241.

Sun, C.L., Lee, H.H., Yang, J.M., Wu, C.C., 2011, Biosens. Bioelectron. 26, 3450.

Szantai, E., Szilagyi, A., Guttman, A., Sasvari-Szekely. M., Ronai, Z., J. 2004, Chromatogr. A 1053, 241.

Wang, X., Hu, C.G., Liu, H., Du, G.J., He, X.S., Xi, Y., 2010, Sensor. Actuat. B 144, 220.

Wang, Z.B., Zuo, P.J., Wang, G.J., Du, C.Y., Yin, G.P., 2008, J. Phys. Chem. C 112, 6582.

Wen, D., Guo, S.J., Dong, S.J., Wang, E.K., 2010, Biosens. Bioelectron. 26, 1056.

Weng, Y.C., Lee, Y.G., Hsiao, Y.L., Lin, C.Y., 2011, Electrochim. Acta 56, 9937.

Wu, G.h., Wu, Y.F., Liu, X.W., Rong, M.C., Chen, X.M., Chen, X., 2012, Anal. Chim. Acta 745, 33.

Wu, T., Guan, Y., Ye, J., 2007, Food Chem. 100, 1573.

Wu, X., Diao, Y., Sun, C., Yang, J., Wang, Y., Sun, S., 2003, Talanta 59, 95.

Zhang, W., Yuan, R., Chai, Y.Q., Zhang, Y., Chen, S.H., 2012, Sens. Actuators B 166–167, 601.

Zhang, Y., Zhang, M., Cai, Z.Q., Chen, M.Q., Cheng, F.L., 2012, Electrochim. Acta 68, 172.

Zhao, Y., Fan, Y.E.L., Qiu, Y., Yang, S., 2007, Electrochim. Acta 52, 5873.

Zuo, X., Zhang, H., Li, N., 2012, Sens. Actuators B 161, 1074.

Figure Captions

Fig. 1. (A) TEM image, (B) HR-TEM image, (C) Selected area diffraction (SAED) pattern and (D) HAADF-STEM image of PdNi nanocrystals. (E) XRD patterns of (a) Pd/C and (b) as-synthesized PdNi/C nanocrystals. (F) EIS of bare GC (a), Pd/C modified GC (b), and PdNi/C modified GC (c) electrodes.

Fig. 2. Cyclic voltammograms of bare GC (a), Pd/C modified GC (b), and PdNi/C modified GC (c) electrodes in 50 mM KOH+ 50 mM PBS containing 10 mM AA. Scan rate: 20 mV s^{-1}.

Fig. 3. (A)CVs of the PdNi/C modified GCE when exposed to 2.0 mM AA in a 50 mM KOH+ 50 mM PBS at different scan rates (from inner to outer): (a)20, (b)40, (c)60, (d)80 and (e)100 mV/s. (B) Plots of anodic peak current vs. $\nu^{1/2}$. (C) Plot of E_p vs. log ν for the oxidation of AA at the PdNi/C modified GCE.

Fig. 4. Amperometric responses of PdNi/C modified GCE at (A) different potentials (-0.40– 0.00 V), and (B) -0.05 V, in stirred 50 mM KOH+ 50 mM PBS with successive addition of AA. The inset is the plot of electrocatalytic current of AA versus its concentrations.

Fig. 5. Interference test of the sensor in 50 mM KOH+ 50 mM PBS at -0.05 V with 0.2 mM AA and other interferents as indicated.

Table 1

Determination of AA in vitamin C tablet, rabbit and goat serum.

Samples	Determined AA (mM)	Added (mM)	Found (mM)	RSD (n = 3, %)	Recovery (%)
Vitamin C tablet	0.21	0.20	0.39	1.9	95.1
		0.40	0.59	1.2	96.7
		0.60	0.80	1.8	98.8
Rabbit serum	0.008	0.02	0.028	1.4	100.0
		0.04	0.051	1.3	106.3
		0.06	0.067	0.9	98.5
Goat serum	0.004	0.02	0.024	1.8	100.0
		0.04	0.045	1.0	102.3
		0.06	0.062	1.1	96.9

Figure(s)

Fig. 1

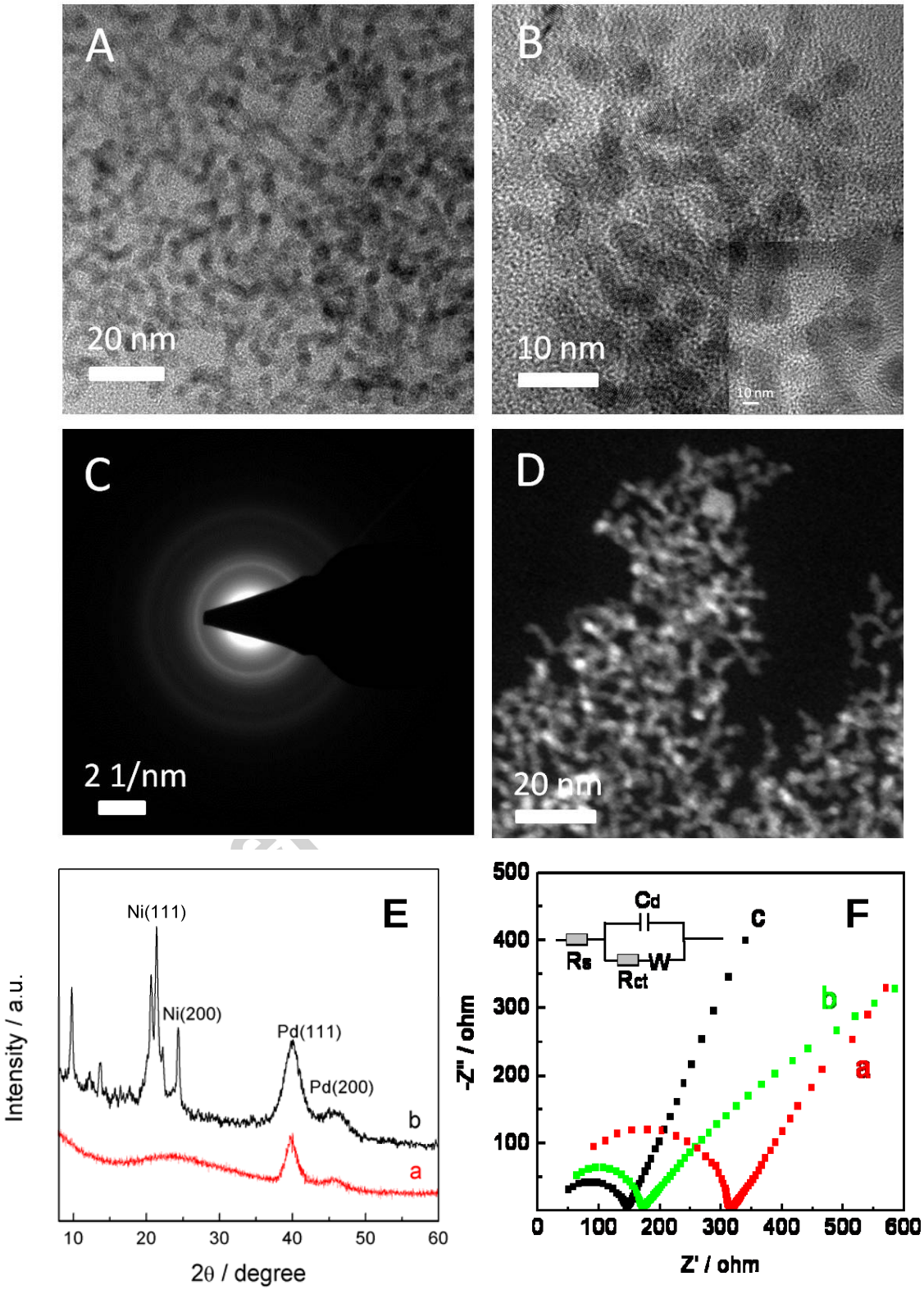

Fig. 2

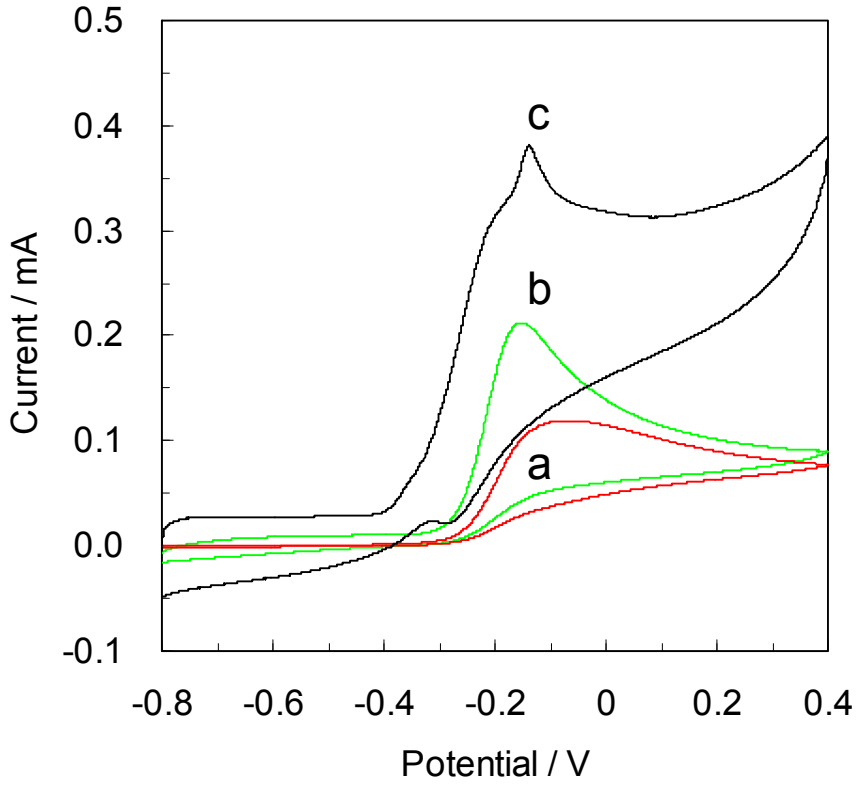

Fig. 3

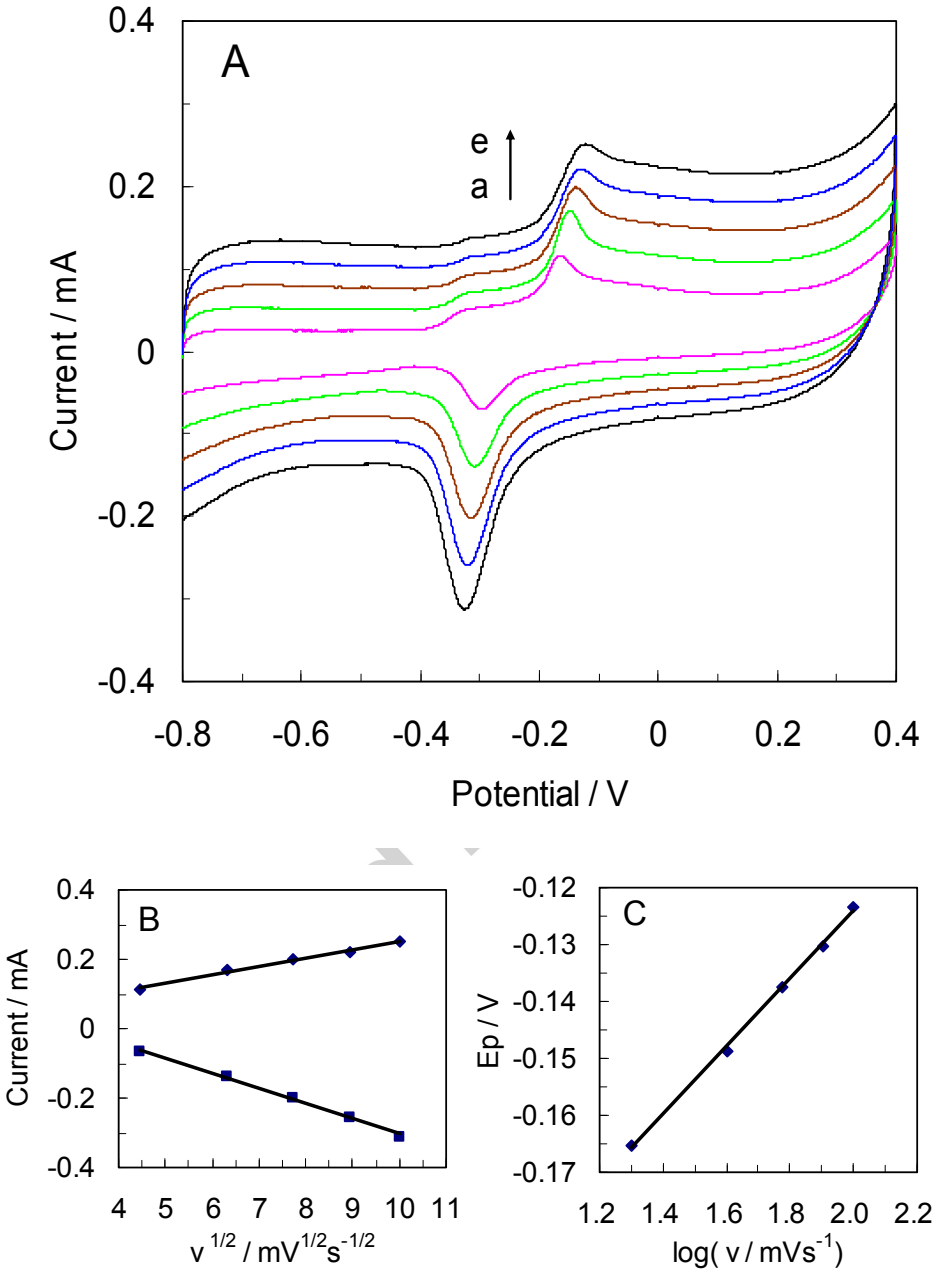

Fig. 4

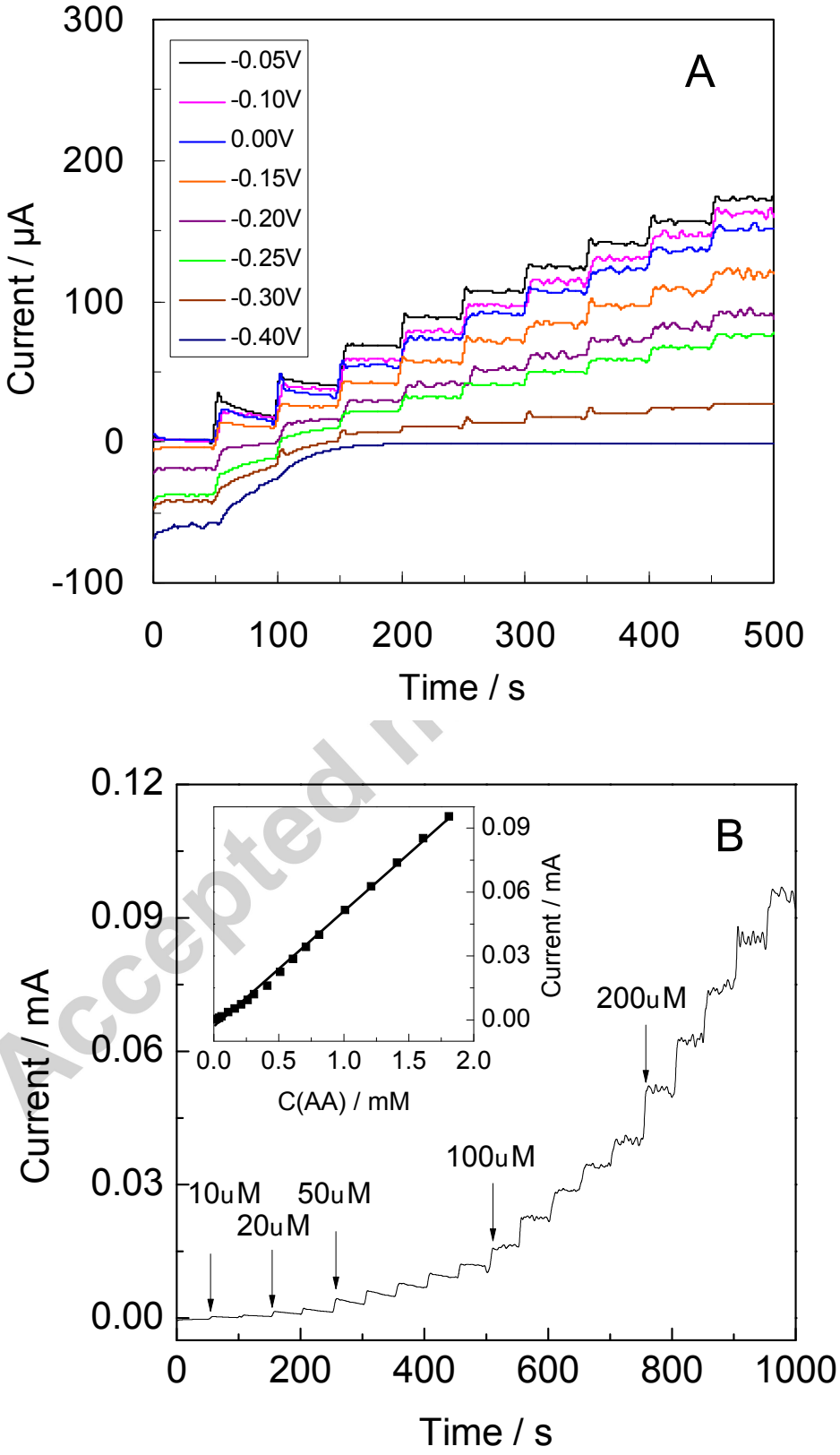

Fig. 5

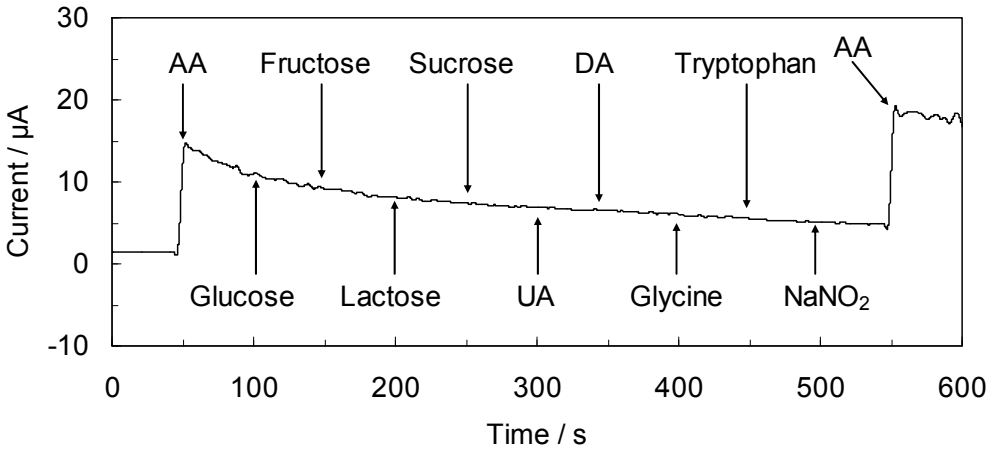

Highlights

- ► Carbon-supported PdNi nanoparticles (PdNi/C) prepared.
- ► A novel synthetic route for PdNi/C preparation.
- ► The performance was better than Pd/C because of the Pd-Ni synergistic effects.
- ► PdNi/C was employed for ascorbic acid determination.
- ► High selectivity, good stability, wide linear range and high sensitivity.